

Nonequilibrium electron transport in strongly correlated molecular junctions

J. E. Han

Department of Physics, State University of New York at Buffalo, Buffalo, NY 14260, USA

(Dated: May 28, 2018)

We investigate models of molecular junctions which constitute minimal Hamiltonians to account for zero-bias-anomaly and the satellite features of inelastic transport by molecular phonons. Through nonlinear transport calculations with the imaginary-time nonequilibrium formalism, a HOMO-LUMO model with Anderson-Holstein interaction is shown to produce co-tunneling conductance peak in the vicinity of Kondo resonance which is mediated by a re-emergent many-body resonance assisted by phonon excitations at bias equal to the phonon frequency. Destruction of the resonance leads to negative-differential-resistance in the sequential tunneling regime.

PACS numbers: 73.63.Kv, 72.10.Bg, 72.10.Di

Strong correlation in nonequilibrium electron transport has emerged as one of the most exciting fields of condensed matter physics. The research in this field so far has been mostly driven by semiconductor-fabricated quantum dots (QDs). The zero-bias anomaly (ZBA) phenomena have been extensively studied in the context of Kondo phenomena [1, 2]. In recent years, similar ZBA phenomenon in molecular junctions [3, 4, 5, 6] has generated tremendous excitement for possible different mechanisms for strongly correlated transport.

Currently, the research on molecular junctions in strongly correlated regime is, both experimentally and theoretically, at an early stage and little is known for the underlying transport mechanisms. One of the most outstanding transport phenomena in molecular devices is the co-existence of the ZBA and the inelastic conductance peaks, presumably due to molecular phonons [3, 4, 5]. Theoretically, the strong correlation in molecular systems poses a great challenge since strong Coulomb and electron-phonon (el-ph) interactions make perturbative approaches unreliable. Only recently, strong correlation physics in the Anderson-Holstein model has been understood for equilibrium systems [7, 8, 9]. Most works on nonequilibrium transport in molecular systems have been perturbative and often excluded Coulomb interaction [10, 11]. Although nonperturbative nonequilibrium theories have seen important breakthroughs [12, 13, 14, 15, 16] in the past few years, the methods have not been adequate to tackle complex models such as molecular junctions.

The main goal of this work is to identify minimal Anderson-Holstein models which can describe the Kondo anomaly and the inelastic features at finite source-drain bias, and reproduce some of experimental findings [3, 4, 5, 6]. We apply the recently developed imaginary-time theory [13] and numerically solve the Anderson-Holstein models via quantum Monte Carlo (QMC) method [17]. Due to the diverse molecular systems, it is very important at this stage to have guiding principles to categorize molecular models for different transport phenomena. The main system of focus here are molecular quantum dots which exhibit the ZBA accompanied by con-

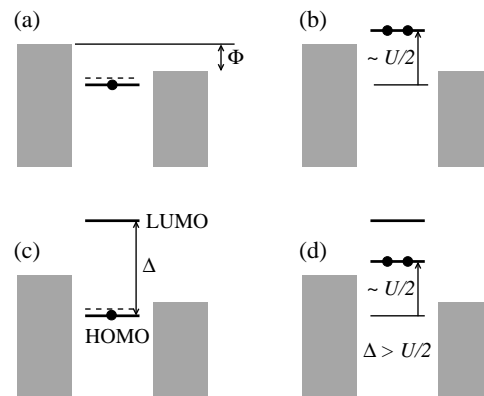


FIG. 1: Schematic energy diagrams for isolated molecular configurations with respect to source/drain reservoirs under bias Φ . (a) Single-orbital model with one electron occupying the level at energy ϵ_d . Phonon excitation level is marked by a dashed line. (b) With an extra electron, the energy level is pushed up $\epsilon_d + U \sim U/2$ by Coulomb repulsion. (c) HOMO-LUMO model with the level spacing Δ . (d) Charge-excited state. With $\Delta \gg U/2$, the LUMO level is nearly empty.

ductance oscillations at bias near the ZBA energy scale, which have been often attributed to the molecular vibrations. This problem, from the strong-correlation point of view, is quite puzzling since near the Kondo anomaly the charge fluctuations are strongly suppressed and phonons which interact with electric charge fluctuations are effectively decoupled [8, 18]. In single-orbital Anderson-Holstein models, it has been shown that phonon spectral features in strong Coulomb limit are weak.

To resolve the issue, we consider two scenarios. First, we note that, at finite bias, the strong correlation effects become weaker, as shown in the disappearance of Kondo peak [1, 2]. Then incoherent charge fluctuations induced by nonequilibrium may enhance the effective el-ph interaction. Within this scenario, we study the single-orbital (SO) Anderson-Holstein model. [See FIG. 1(a-b)] Second, we study a two-orbital model with highest-occupied-molecular-orbital (HOMO) and lowest-unoccupied-molecular-orbital (LUMO). Despite being

more realistic, HOMO/LUMO (HL) models have not been extensively studied due to their complexity. Multiple orbitals allow the electron density distortion to couple to molecular distortions, *i.e.* molecular Jahn-Teller (JT) modes, without invoking on-site charge fluctuations. It has been shown that in strong correlation limit [8], the JT coupling becomes very effective. [See FIG. 1(c-d)]

For both models, the electron source/drain reservoirs are modeled by the Hamiltonian $H_c = \sum_{k\alpha\sigma} \epsilon_{\alpha k\sigma} c_{\alpha k\sigma}^\dagger c_{\alpha k\sigma}$ in terms of the electron creation (annihilation) operator $c_{\alpha k\sigma}^\dagger$ ($c_{\alpha k\sigma}$) with k the continuum index, σ spin index, and the reservoir index $\alpha = \pm 1$ for source (L) and drain (R), respectively. The charge part of the QD Hamiltonian for the single-orbital model is

$$H_{ch,SO} = \epsilon_d \sum_{\sigma} n_{d\sigma} + \frac{U}{2} (n_{d\uparrow} + n_{d\downarrow} - 1)^2, \quad (1)$$

with the number operator $n_{d\sigma} = d_{\sigma}^\dagger d_{\sigma}$ of the QD orbital d_{σ}^\dagger , the level energy ϵ_d and the Coulomb parameter U . The Holstein phonon and the el-ph coupling for the SO model can be written as

$$H_{ph,SO} = \omega_{ph} a^\dagger a + g_{ep} (a^\dagger + a) (n_{d\uparrow} + n_{d\downarrow} - 1), \quad (2)$$

with a^\dagger for creation of phonon, ω_{ph} the phonon frequency, g_{ep} the el-ph coupling constant. The tunneling part is $H_{t,SO} = -t \sum_{\alpha k\sigma} (d_{\sigma}^\dagger c_{\alpha k\sigma} + h.c.)$ with the hopping parameter t . Here the tunneling rate is parametrized by the hybridization function $\Gamma_{L,R} = \pi t^2 N(0)$ with $N(0)$ the density of state of the reservoirs. Throughout this work, we assume $\Gamma_L = \Gamma_R$ and use $\Gamma = \Gamma_L + \Gamma_R = 1$ as the unit of energy. The total Hamiltonian is $H = H_c + H_t + H_{ch} + H_{ph}$. Here, we study the regime where the phonon frequency is comparable to the Kondo temperature and we set $\omega_{ph} \sim \Gamma$, in contrast to semiconductor QD models where the phonon-excited QD-levels are discrete and well-defined ($\omega_{ph} > \Gamma$) [19].

We solve steady-state nonequilibrium using the imaginary-time formalism [13]. This method combines the nonequilibrium quantum statistics and quantum dynamics within the equilibrium theory via an imaginary-time Hamiltonian with complex chemical potentials parametrized by the *Matsubara voltage* $\varphi_m = 4\pi mT$ as

$$\hat{K}(i\varphi_m) = \hat{K}_0(i\varphi_m) + \hat{V} = \hat{H}_0 + \frac{1}{2}(i\varphi_m - \Phi)\hat{Y}_0 + \hat{V}, \quad (3)$$

where the many-body interaction is given by \hat{V} and the non-interacting part by $\hat{H}_0 = H_c + H_t + \epsilon_d \sum_{\sigma} n_{d\sigma}$. Population of the scattering states for source and drain in the non-interacting limit is imposed by the operator [12, 20] $\hat{Y}_0 = \sum_{k\sigma} (\psi_{Lk\sigma}^\dagger \psi_{Lk\sigma} - \psi_{Rk\sigma}^\dagger \psi_{Rk\sigma})$, with the scattering state operator $\psi_{\alpha k\sigma}^\dagger$ from the α -reservoir [20]. \hat{Y}_0 can be exactly solved in the non-interacting limit. In a perturbation expansion with \hat{V} , the quantum statistics is unaffected by $i\varphi_m$ due to $e^{-\beta K_0} = e^{-\beta(H_0 - \frac{\Phi}{2}Y_0)}$, since

$\frac{1}{2}\beta\varphi_m\hat{Y}_0$ represents $2\pi \times (\text{integer})$ with respect to the unperturbed scattering-state basis. The quantum dynamics, represented by an energy denominator in Green functions, is recovered by the analytic continuation $i\varphi_m \rightarrow \Phi$. This formalism can be shown to be equivalent to the retarded Green function in the Keldysh formalism.

With this formalism, the equilibrium auxiliary-field QMC method [17] can be immediately applied with $K(i\varphi_m)$ as the Hamiltonian. The resulting self-energy $\Sigma(i\omega_n, i\varphi_m)$ at the fermion Matsubara frequency $\omega_n = (2n+1)\pi T$ should be analytically continued numerically. This is achieved by making an ansatz on the spectral representation [13],

$$\Sigma(i\omega_n, i\varphi_m) = a(i\varphi_m) + \sum_{\gamma} \int \frac{\sigma_{\gamma}(\epsilon) d\epsilon}{i\omega_n + \frac{\gamma}{2}(i\varphi_m - \Phi) - \epsilon}, \quad (4)$$

with the spectral function $\sigma_{\gamma}(\epsilon)$. The index γ of odd integer is a combination of reservoir indices α in particle-hole lines in a self-energy diagram. This representation is exact in the equilibrium limit or in the second order perturbation in nonequilibrium. We use $\sigma_{\gamma}(\epsilon)$ as fitting parameters to the numerical self-energy. In the particle-hole symmetric case, the ω_n -independent term $a(i\varphi_m)$ is zero. With particle-hole asymmetry, we use a simple-pole approximation $a(i\varphi_m) = a_0 + a_1[(i\varphi_m - z)^{-1} + (-i\varphi_m - z^*)^{-1}]$, with fitting parameter a_0, a_1, z with $\text{Im } z < 0$ for $\varphi_m > 0$. $a(i\varphi_m)$ has a weak dependence on φ_m and the analytic continuation has been insensitive to the choice of a fitting form. Once all the fitting parameters are found, we set $i\varphi_m \rightarrow \Phi$ and $i\omega_n \rightarrow \omega + i\eta$, and obtain the retarded self-energy and QD Green function $G^{ret}(\omega)$. The current is calculated from

$$I = \frac{2e}{h} \int d\omega \pi \Gamma A(\omega) \left[f\left(\omega - \frac{\Phi}{2}\right) - f\left(\omega + \frac{\Phi}{2}\right) \right], \quad (5)$$

with $A(\omega) = -\pi^{-1} G^{ret}(\omega)$ [21].

The differential conductance $G = e(dI/d\Phi)$ for the SO model is shown in FIG. 2 in the particle-hole symmetric limit $\epsilon_d = -U/2$. At $U = 0$, the system has a ZBA peak with the HWHM ($\Phi_{HWHM} \sim 0.3$), much reduced from the non-interacting value $\Phi_{HWHM}^0 = 2$, demonstrating the charge-Kondo effect [9, 22]. As U approaches the el-ph binding energy $2g_{ep}^2/\omega_{ph}$, the correlation effect becomes weaker indicating the competition of the attractive el-ph and repulsive Coulomb interactions. As U grows further, the system approaches the usual spin-Kondo regime. The fine structure in the conductance shows faint oscillations, reminiscent of some of the experiments [5]. However, given the numerical uncertainties, we cannot conclude that the features are a direct manifestation of inelastic excitation of phonon quanta. In an extensive set of calculations we found no well-defined phonon satellites near the ZBA energy scale. To further support the idea, we doubled the phonon frequency

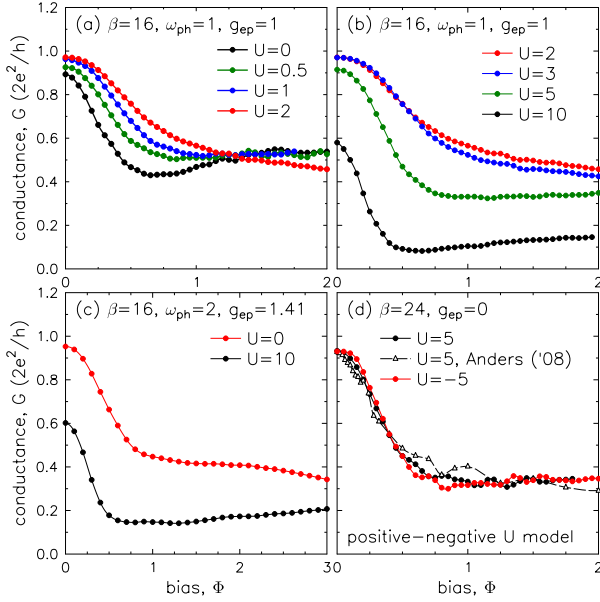


FIG. 2: (Color online) Differential conductance in single-orbital Anderson-Holstein model. (a) Conductance with large el-ph coupling ($2g_{ep}^2/\omega_{ph} > U$) in the charge-Kondo regime. As U increases from zero, correlation effects become weaker. (b) Spin-Kondo regime recovered with large U . (c) Larger phonon frequency at fixed $g_{ep}^2/\omega_{ph} = 1$. (d) Comparison of the $g_{ep} = 0$ limit to Ref [14] and the negative U model. The unit of energy is the non-interacting line-broadening Γ .

($\omega_{ph} = 2$) at fixed g_{ep}^2/ω_{ph} . FIG. 2(c) shows similar results as (a-b) with weaker fine structures, possibly from more efficient QMC sampling at high ω_{ph} . We conclude that the main effect of el-ph interaction in the SO model is the reduction of the Coulomb interaction and that the conductance at high bias is more related to the el-ph scattering than to the energy exchange with phonon.

FIG. 2(d) shows results from pure Anderson models. In the previous work of Han and Heary [13], the particle-hole symmetry condition on the spectral function in Eq. (4), $\sigma_\gamma(\epsilon) = \sigma_{-\gamma}(-\epsilon)$, was not properly imposed and they obtained underestimated ZBA peak-widths. A modified fit gives an improved agreement with Ref. [14]. We also test the idea whether the nonequilibrium imposed on the charge variable as opposed to the spin variable has any significant effects on the nonlinear transport. The positive-negative U models are interchangeable in equilibrium [22] by switching the charge and spin variables. The calculation shows that the difference between the two models even at high bias is minimal.

We now turn to the HOMO/LUMO model. We denote the QD levels by $d_{i\sigma}^\dagger$ with $i = 1, 2$ for HOMO and LUMO, respectively. The charge part of the Hamiltonian is

$$H_{ch,HL} = \sum_{\sigma,i=1,2} \epsilon_i n_{i\sigma} + \frac{U}{2} (n_{1\uparrow} + n_{1\downarrow} - 1)^2, \quad (6)$$

with the HOMO level at $\epsilon_1 = \epsilon_d$, the LUMO level at $\epsilon_2 = \epsilon_d + \Delta$. The Coulomb interaction is set to act only on the HOMO level, since the inclusion of the LUMO led to severe sign-problems in QMC calculations. However, in the following calculations, the negligence of Coulomb interaction on the LUMO becomes a reasonable approximation since we choose the level spacing Δ much larger than the charging energy ($\Delta \gg \frac{U}{2}$) such that the LUMO level is mostly empty. (See FIG. 1)

We model the el-ph coupling via the Jahn-Teller phonons of a_m^\dagger ($m = 1, 2$) as

$$H_{ph,HL} = \omega_{ph} \sum_m a_m^\dagger a_m + \sum_{ijm\sigma} (a_m^\dagger + a_m) d_{i\sigma}^\dagger V_{ij}^{(m)} d_{j\sigma}, \quad (7)$$

with the 2×2 JT coupling matrix [23] given as $V^{(1)} = g_{ep} \hat{\sigma}_z$, $V^{(2)} = g_{ep} \hat{\sigma}_x$, with the Pauli matrices $\hat{\sigma}_z$ and $\hat{\sigma}_x$. The second phonon ($m = 2$) makes direct electronic transitions between the LUMO and HOMO without tunneling through reservoirs. The tunneling part is given as $H_{t,HL} = -t \sum_{\alpha k \sigma} \sum_i (d_{i\sigma}^\dagger c_{\alpha k \sigma} + h.c.)$. The average sign in the QMC calculations has been moderate at $Sign = 0.5 - 1.0$.

The conductance in FIG. 3 shows clear phonon excitation peaks at $\Phi = \omega_{ph}$. The HOMO-LUMO level spacing is set at $\Delta = 15$, much greater than any other energy scales. With the HOMO level at $\epsilon_d = -1.1$, the HOMO occupation number $n_{HOMO} \sim 0.57$ at $\Phi = 0$ for (a). For (c), $\epsilon_d = -1.5$ and $n_{HOMO} \sim 0.48$. The main features of the conductance are the ZBA and the peak at $\Phi \approx \omega_{ph}$.

To understand how the co-tunneling via phonon excitation arises, we study the QD spectral function as $\Phi \rightarrow \omega_{ph}$. In FIG. 2(b), spectral functions are plotted for $\Phi = 0, \dots, 1$ with the interval of 0.2. Curves are off-set for clarity. Destruction of the ZBA resonance is similar to the pure Anderson models [13, 14]. At $\Phi = 0$, the other dominant peak is the charge excitation peak, marked by A in (b). As Φ grows, the peak A quickly migrates to the peak B at $\omega = \omega_{ph}$ for phonon excitation. The peak B is not directly responsible for the conductance peak at $\Phi = \omega_{ph}$ since the peak B is outside the transport energy window $[-\Phi/2, \Phi/2]$ in Eq. (5).

The co-tunneling transport is carried by a new emerging resonance as indicated by peak C in FIG. 3(b). As the ZBA peak disappears, another resonance peak inside the transport energy window becomes stronger. At $\Phi = \omega_{ph}$, the mismatch of electron Fermi energies from the source and drain is compensated by an emission of a phonon quantum. Then effectively the same electronic chemical potentials on both reservoirs seem to result in a Kondo-like phonon-assisted many-body resonance.

In a pure phonon model in FIG. 3(c-d), the conductance behavior remains qualitatively the same, but it showed a strong negative-differential-resistance (NDR) behavior near $\Phi/2 \approx \omega_{ph}$ in the inelastic sequential tunneling regime. As shown in a dashed line at $\Phi = 2\omega_{ph}$,

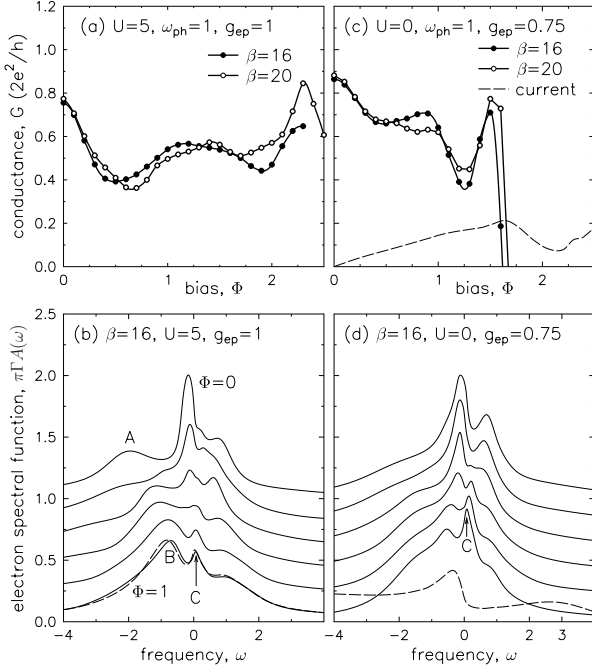


FIG. 3: Differential conductance in the HOMO-LUMO model with Anderson-(Jahn-Teller) Holstein model. (a) Conductance peaks for the Kondo anomaly and inelastic co-tunneling at $\Phi = \omega_{ph}$. (b) Spectral functions for bias $\Phi = 0, \dots, 1$ with the interval 0.2. Curves are shifted for clarity. With increasing Φ , the Kondo peak disappears and the Coulomb peak (peak A) shifts to phonon excitation energy (peak B). As $\Phi \rightarrow \omega_{ph}$, new resonance (peak C) emerges inside the voltage window and contributes to the co-tunneling conductance peak at $\Phi \approx \omega_{ph}$. Dashed line is for $\beta = 20$. (c) Conductance in pure el-ph limit. A strong negative-differential-resistance (NDR) effect appears at $\Phi/2 = \omega_{ph}$ in the sequential tunneling regime. (d) Disappearance of the resonance (dashed line at $\Phi/2 = \omega_{ph}$) leads to the NDR.

the spectral weight shifts to high frequency and the resonance peak C is destroyed, which leads to the NDR. Similar polaronic effects to NDR in molecular systems have been reported previously [24]. Although this behavior is robustly reproduced at different parameters, it should be mentioned that this is the regime where the ansatz, Eq. (4), starts to deviate from the QMC data significantly and vertex corrections may be necessary.

Finally, nonequilibrium-induced multi-phonon modes are shown in FIG. 4. The phonon spectral functions are calculated by the same ansatz, Eq. (4), but with even integers γ . At $\Phi = 0$, the phonon frequency is highly renormalized from ω_{ph} , but phonons are mostly in the lowest quantum state. As Φ increases, the spectral weight transfers to multiple phonon modes as previously predicted [10, 11].

I thank useful discussions with F. Anders, H. van der Zant, R. Heary. I acknowledge support from the Na-

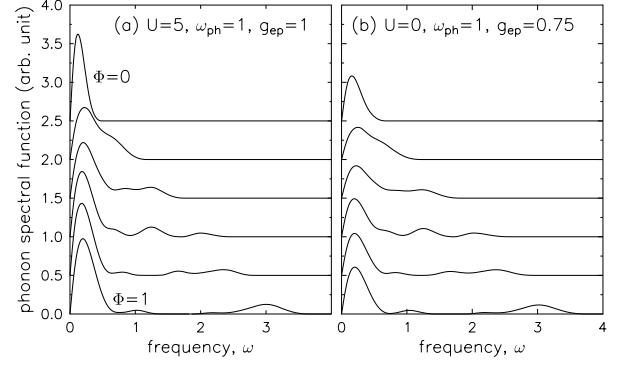


FIG. 4: (a) Phonon spectral function of HOMO/LUMO model for parameters of FIG. 3(a). At $\Phi = 0$, phonon is strongly renormalized. With increasing Φ , higher phonon quanta are created by absorbing the chemical potential difference in the electron reservoirs. (b) Similar results for FIG. 3(b).

tional Science Foundation DMR-0426826 and computing resources at CCR of SUNY Buffalo.

-
- [1] S. M. Cronenwett, T. H. Oosterkamp, L. P. Kouwenhoven, *Science* **281**, 540 (1998); W. G. van der Wiel, *et al.*, *Science* **289**, 2105 (2000).
 - [2] M. Grobis *et al.*, *Phys. Rev. Lett.* **100**, 246601 (2008).
 - [3] L. H. Yu and D. Natelson, *Nano Lett.* **4**, 79 (2004).
 - [4] L. H. Yu *et al.*, *Phys. Rev. Lett.* **93**, 266802 (2004).
 - [5] E. A. Osorio *et al.*, *Nano Lett.* **7**, 3336 (2007).
 - [6] G. D. Scott *et al.*, arXiv.org:0904.2575v1 (2009).
 - [7] A.C. Hewson and D. Meyer, *J. Phys.:Cond. Matter* **14**, 427 (2002).
 - [8] J. E. Han, O. Gunnarsson and V. H. Crespi, *Phys. Rev. Lett.* **90**, 167006 (2003).
 - [9] P. S. Cornaglia, H. Ness, and D. R. Grempel, *Phys. Rev. Lett.* **93**, 147201 (2004).
 - [10] A. Mitra, I. Aleiner, and A. J. Millis, *Phys. Rev. Lett.* **94**, 076404 (2005).
 - [11] K. Flensberg, *Phys. Rev. B* **68**, 205323 (2003).
 - [12] S. Hershfield, *Phys. Rev. Lett.* **70**, 2134 (1993).
 - [13] J. E. Han and R. J. Heary, *Phys. Rev. Lett.* **99**, 236808 (2007).
 - [14] F. B. Anders, *Phys. Rev. Lett.* **101**, 066804 (2008).
 - [15] N. Shah and A. Rosch, *Phys. Rev. B* **73**, 081309(R) (2006).
 - [16] P. Mehta and N. Andrei, *Phys. Rev. Lett.* **96**, 216802 (2006).
 - [17] R. M. Fye and J. E. Hirsch, *Phys. Rev. B* **38**, 433 (1988).
 - [18] G. Sangiovanni *et al.*, *Phys. Rev. Lett.* **94**, 026401 (2005).
 - [19] R. Lake and S. Datta, *Phys. Rev. B* **45**, 6670 (1992).
 - [20] J. E. Han, *Phys. Rev. B* **73**, 125319 (2006); J. E. Han, *Phys. Rev. B* **75**, 125122 (2007).
 - [21] Y. Meir and N. S. Wingreen, *Phys. Rev. Lett.* **68**, 2512 (1992).
 - [22] A. Taraphder and P. Coleman, *Phys. Rev. Lett.* **66**, 2814

- (1991).
- [23] N. Manini, E. Tosatti, and A. Auerbach, Phys. Rev. B **49**, 13008 (1994).
- [24] M. Galperin, M. A. Ratner, and A. Nitzan, Nano Lett. **5**, 125 (2005).